

REGIONAL SCALE LITHOLOGIC MAPPING IN WESTERN TIBET USING ASTER THERMAL INFRARED MULTISPECTRAL DATA

Y. Ninomiya ^{a,*}, B. Fu ^b

^a Geological Survey of Japan, AIST, Tsukuba, Japan – yoshiki.ninomiya@aist.go.jp

^b Institute of Geology and Geophysics, CAS, Beijing, China

KEY WORDS: ASTER, Thermal Infrared, Lithologic mapping, Mineralogic indices, Quartz, Carbonate, Ultramafic, Tibet

ABSTRACT:

Lithologic mapping in the hostile and inaccessible mountainous region like the Himalaya and Tibet has frequently been a great challenge for geologists. The remote sensing techniques should be a potential player in lithologic mapping and structural analysis in these mountainous regions. With the successful development of mineralogic indices, e.g., Quartz Index (QI), Carbonate Index (CI), Mafic Index (MI) based on the ASTER multispectral thermal infrared (TIR) data, which have demonstrated the usefulness and effectiveness of ASTER TIR data on lithologic mapping in the semi-arid to arid regions, we began to develop a lithologic mapping system since 2005. The system can store some necessary information for data searching and provide a priority order determination for the scenes covering the specified region. Also, it can calculate the mineralogic indices and generate the lithologic mapping images to cover the target region. This lithologic mapping system was successfully applied to lithologic mapping in some target regions in western China. We employ continuously ASTER TIR multispectral data for lithologic mapping in the western Tibetan Plateau, in which the geologic mapping is a great challenge for the human beings because the average elevation in this region is over 5000 m above sea level in 2009 JFY. Here, we show the regional scale lithologic mapping result. Detailed lithologic mapping and geologic analysis of ASTER multispectral data in this region will improve our understanding of the evolution of the India-Asia collision.

1. INTRODUCTION

ASTER (Advanced Spaceborne Thermal Emission and Reflection Radiometer) instrument (Fujisada, 1995; Yamaguchi et al., 1998), launched in December 1999 onboard the Terra satellite, is the first and the only satellite-borne imaging sensor with a capability of multispectral observation in the thermal infrared (TIR; 8 to 12 microns) spectral region at spectral, radiometric and spatial resolutions adequate for geological studies. For an overview of ASTER, it is directed to the paper in this abstract volume (Corrie et al., 2010). Most of the methods for lithologic or mineralogic mapping with multispectral TIR remote sensing data proposed so far premises to apply emissivity data as input, but methods applying Level-1B radiance at the sensor data without atmospheric corrections have an advantage in data productivity. Another advantage of the methods for Level-1B is the extendibility for Level-3A data, enables easy fusion with GIS. The authors proposed Quartz Index (QI), Carbonate Index (CI) and Mafic Index (MI) which closely correlates to the bulk SiO₂ content, for ASTER TIR data with theoretical and practical analyses for the applicability of Level-1B data, improved the indices, and showed that the lithologic mapping with the indices for Level-1B data can be stable against the variation of temperature and atmospheric conditions (Ninomiya, 2002; Ninomiya, 2003; Ninomiya, 2004; Ninomiya et al., 2005).

The study area covers the western part of the Indus-Yarlung Zangbo Suture Zone (IYSZ) (also called Indus-Tsangpo). IYSZ is mainly composed of remnants of the Neo-Tethys ocean-floor and marks a major suture between the Indian Plate, to the south, and the Lhasa Block of Tibet, to the north. The IYSZ is thus the southernmost and the youngest of the sutures that divide the Tibetan Plateau into various E–W terranes (Figure 1). It is characterized by a more or less continuous ophiolitic chain (Figure 1b). The IYSZ ophiolites and adjacent sedimentary formations were first thrust (obducted) to the south onto the Indian continent, then backthrust to the north and finally

affected by strike-slip and late E–W extensional events (Molnar and Tapponnier, 1975; Tapponnier et al., 1981; Yin and Harrison, 2000).

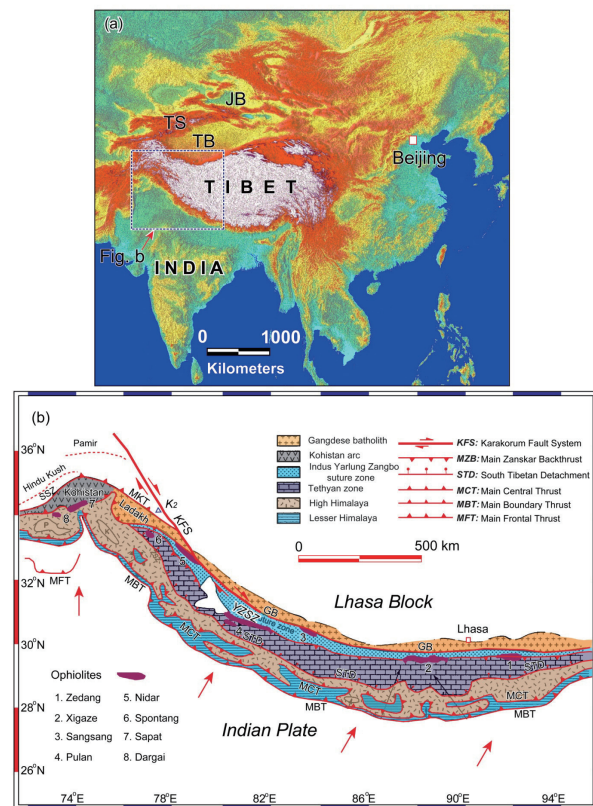


Figure 1 (a) Topographic map of the India-Asia collision zone. (b) Geologic sketch map of the Himalaya showing the Indus-Yarlung Zangbo suture zone and ophiolite complexes (modified from Gansser, 1981; Windley, 1983).

* Corresponding author.

Along the suture, major crustal discontinuities (Mesozoic and Cenozoic thrust fault systems) delimit three main tectonic units of different geologic, deformational and metamorphic histories (e.g. Burg et al., 1987; Hodges, 2000). These units are, from north to south, the active paleomargin (components of the Andean-type southern margin of the Lhasa Block), the oceanic domain (components of the Neo-Tethys ocean-floor, i.e. ophiolitic sequences) and the passive paleomargin (components of the northern passive margin of the Indian plate). The ophiolitic sequences, including the ophiolitic melange, are thus fault-bounded to the north by the forearc Xigaze Group and the Gangdese batholith, and to the south by the Mesozoic Yamdrock Me'lange and Triassic flysch (Figure 1b).

2. METHODOLOGY

2.1 Mineralogic indices defined for ASTER TIR

Several mineralogic indices, Quartz Index (QI), Carbonate Index (CI) and Mafic Index (MI) are defined for ASTER TIR Level-1B radiance at the sensor data without atmospheric correction, based on an analysis of TIR spectral characteristics of rocks and minerals (Ninomiya et al., 2005). They are calculated as shown below.

$$QI = \frac{Band_{11} \times Band_{11}}{Band_{10} \times Band_{12}} \quad (1)$$

$$CI = \frac{Band_{13}}{Band_{14}} \quad (2)$$

$$MI = \frac{Band_{12} \times Band_{14} \times Band_{14} \times Band_{14}}{Band_{13} \times Band_{13} \times Band_{13} \times Band_{13}} \quad (3)$$

Especially for CI, it is heavily affected by the surface temperature variation. To correct for this, the original ASTER Level-1B data are normalized by converting the brightness temperature at ASTER band₁₃ to a fixed temperature of 300 K using Planck's law (Ninomiya, 2002; Ninomiya, 2003; Ninomiya, 2004; Ninomiya et al., 2005), and applied for the calculation of the mineralogic indices shown above. The normalized radiance at the sensor is calculated as follows:

$$nL_{sat_i} = L_{sat_i} \times \frac{e^{\left\{ \frac{\lambda_{13} \times \ln \left(\frac{c_1}{\pi \times (\lambda_{13})^5 \times L_{sat_{13}} + 1} \right) \right\}} - 1}{e^{\left(\frac{c_2}{\lambda_i \times nT} / \epsilon_{13} \right)} - 1} \quad (4)$$

where, L_{sat_i} = at-sensor spectral radiance in band_i
 λ_i = centre wavelength of band_i (μm)
 c_1 = constant 1 = $3.742 \times 10^8 \text{ W m}^{-2} \mu\text{m}^4$
 c_2 = constant 2 = $1.439 \times 10^4 \mu\text{m K}$
 nT = fixed temperature in Kelvin = 300 K
 ϵ_{13} = emissivity in band₁₃ = 1.0

The emissivity in band 13 is assumed to be unity. For the details of the mineralogic indices and the normalization of the ASTER Level-1B data, the reader is directed to the papers by Ninomiya shown above and a paper in this abstract volume (Corrie et al., 2010).

2.2 ASTER lithologic mapping system

To achieve an effective data processing using the vast and still increasing ASTER data scenes, we have developed a lithologic mapping system. This system is mainly composed of database

and image processing subsystems. The former subsystem can store all the necessary information for data searching, data processing and providing a priority order determination for the scenes covering the specified target region. The latter subsystem can calculate the mineralogic indices and generate the lithologic mapping mosaic images to cover the target region.

The database stores the necessary information for the data processing of each ASTER data retrieved from the ASTER header information including the geo-coordinates of the data coverage. Additionally, it stores the information of the meteorological atmospheric water vapor content at the time of the ASTER observation. It is calculated by interpolating the archived data of the precipitable water included in the six hourly NCAR reanalysis dataset published by NCEP (National Centers for Environmental Prediction), NOAA. It is one of the most useful guideline for judging the quality of the ASTER data in applying the mineralogic indices for mapping because the most affective and the most variable atmospheric factor on the multispectral TIR remote sensing data like ASTER-TIR is the atmospheric water vapor content, although both the accuracy and the spatial resolution of the NCEP data of the precipitable water are very rough. As a guideline, it is high possibility of the acceptable quality for the mapping if the precipitable water is less than 10 kg/m^2 , and non-acceptable quality if it is more than 20 kg/m^2 .

2.3 Procedure to make mosaic lithologic map

The mosaic lithologic map of the mineralogic indices, QI, CI and MI, covering a target area is basically generated with the steps as follows:

1. Searching with the lithologic mapping system, all the ASTER data covering the target area is added to the project.
2. The priority for each ASTER data is temporary determined as the ascending order of the atmospheric water vapor content.
3. Checking the ASTER VNIR image of each data visually, especially for the clouds and snow covers, it is determined to keep in the project or omit from the project.
4. Checking the CI image of each data visually, because CI is very sensitive to the atmospheric water content including clouds and mists which may be not detected in the VNIR image. Then, it is determined to keep in the project or omit from the project.
5. Repeating the steps 3 and 4 necessary times and adjusting the priority order of each ASTER data, the priority order of each ASTER data in the project is finalized.
6. The mosaic map of the mineralogic indices, QI, CI and MI, is generated.

The calculated mineralogic indices are multiplied with a factor of 10,000 and the generated mosaic image of the mineralogic indices are stored in the GeoTIFF form of 16bit integer to avoid the information loss of the calculated values of the mineralogic indices.

3. RESULT AND DISCUSSION

The target region is along the Karakorum fault system (KFS) in the western part of the Indus-Yarlung Zangbo Suture Zone (IYSZ). The region is divided into the tiles of 1 degree by 1 degree coverage in latitude and longitude, and the mosaic lithologic mapping with the mineralogic indices is made for

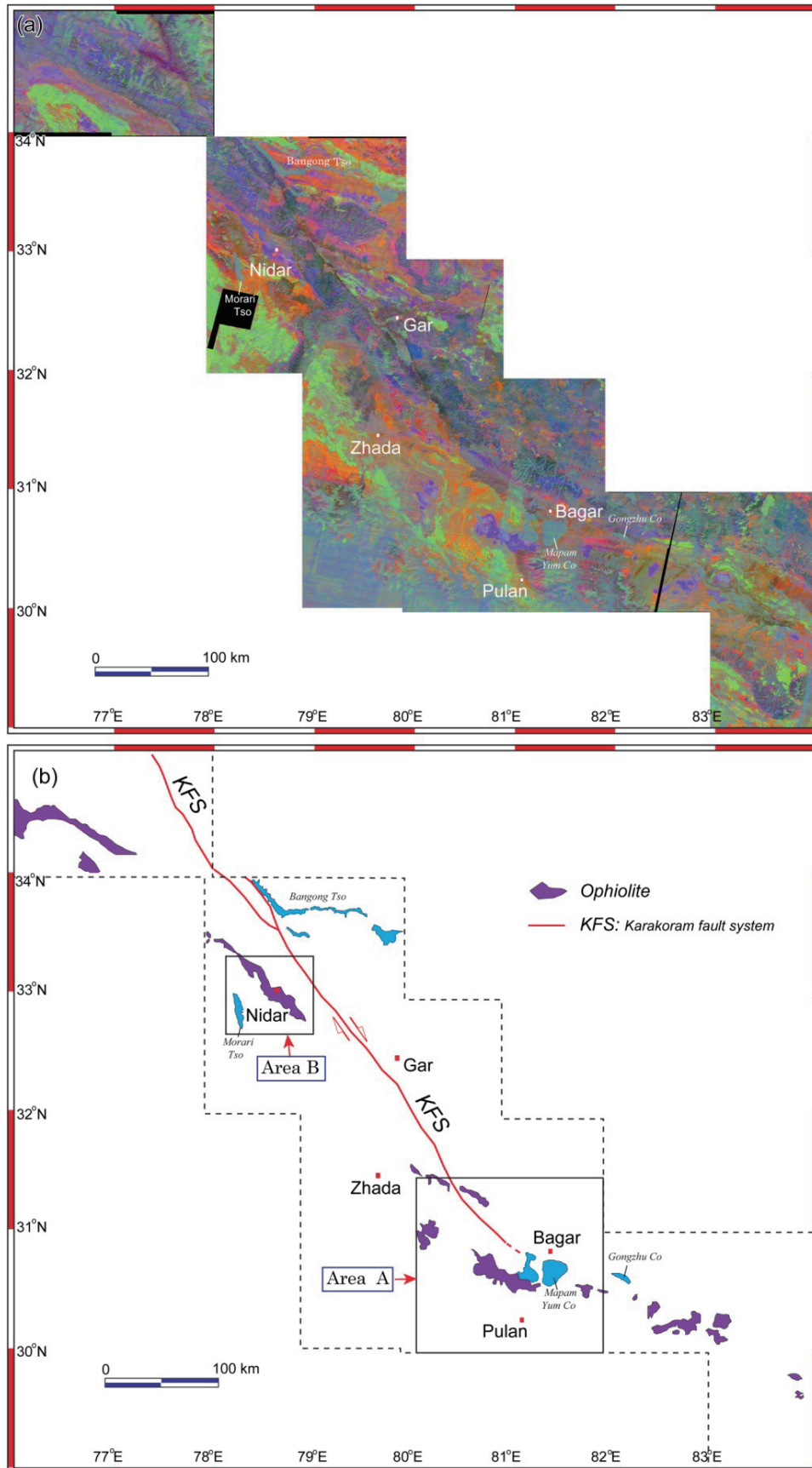


Figure 2 (a) ASTER false-color composite image of QI, CI and MI showing lithologic units in the west segment of IYSZ. (b) Spatial distribution of ophiolite rocks along the western segment of the Indus-Yarlung Zangbo suture zone derived from the ASTER TIR indices image.

each tile in interest using the lithologic mapping system. After that, all the tiles in interest are totally mosaicked furthermore for the regional lithologic mapping.

Usually, each of the indices, QI, CI and MI, is printed as grayscale image by a linear contrast stretch of 1.0 to 1.05, 1.01 to 1.045, and 0.8 to 0.9, respectively, for enhancing the image and interpreting the result. Also, false-color composite image is printed by assigning QI for red, CI for green and MI for blue.

Figure 5 (a) shows the result of a regional scale lithologic mapping as a false-color composite (FCC) image of QI, CI and MI with a linear contrast stretch of 0.97-1.055 (QI; Red), 1.005-1.055 (CI; Green), and 0.79-0.95 (MI; Blue). Basically, quartz rich and feldspar poor rocks, a typical kind of sedimentary rocks, represent light reddish color in the FCC image because of the high QI and low MI signal. Typical feldspar and sulfate minerals have an opposite spectral feature of quartz in ASTER band 10 to 12 spectral region, and feldspar rich rocks or sulfate rich rocks show quite low QI even if it also contains considerable amount of quartz. Feldspar rich rocks, typically granitoids, represent deep bluish to greenish color, and rocks rich in sulfates, typically gypsum or barite, represent deep greenish color in the FCC image of the indices. The major carbonate minerals, calcite and dolomite, show quite high CI, and the typical marine sedimentary rocks represent light greenish color in the FCC image because of the high CI. It should be cared for the confusion that CI is also quite sensitive to atmospheric anomalies with higher water content. Ultramafic minerals show quite high MI, and ultramafic rocks usually represent light purplish color in the FCC image. Some type of salt deposit show quite high MI like ultramafic rocks. Other type of silicate rocks, typically igneous rocks except ultramafic rocks, usually show bluish color because of the relatively high MI compared with QI and CI.

Figure 5 (b) shows the spatial distribution of rock bodies with quite high MI expected as ophiolite rocks along the western segment of the Indus-Yarlung Zangbo suture zone derived from the ASTER-TIR indices image. Although the geological knowledge of the region is very limited because here is a hostile and inaccessible mountainous, some small areas with relatively easy accessibility are well studied and also our field investigation and sampling are limited to along the main road in a part of this region. The lithologic mapping result basically agrees well to the known geology. It is expected that this kind of regional scale lithologic mapping covering vast western China and surrounding region widely include Tibet, or other regions of the earth, will help us a better recognition of the spatial distribution of typical rock types, especially ultramafic ophiolite rocks, and supply a basic data for a better understanding of the regional tectonic evolution history and the other geological topics.

4. CONCLUSION

Satellite remote sensing methods are a powerful tool for detailed geologic analysis, especially in inaccessible regions of the earth surface. ASTER TIR bands are shown to provide spectral information bearing on the lithologic, structural, and geochemical character of rock bodies such as ophiolite. Most remote sensing data are widely available for little or no cost. Mineralogical indices, e.g., Quartz Index (QI), Carbonate Index (CI), Mafic Index (MI) based on TIR spectral properties of the corresponding minerals and rocks, have been successfully developed for ASTER data, which have demonstrated the

usefulness and effectiveness of ASTER TIR data on lithologic mapping in the semi-arid to arid regions. During the operation of ASTER for more than 10 years, enormous data covering the most of earth surface have been acquired. However, how to use such vast and still increasing ASTER data sufficiently for geological application is another tremendous challenge for geoscientists. Therefore, we have developed a lithologic mapping system for ASTER multispectral TIR data. For a very wide target area compared to the coverage of single ASTER data, the western margin region of Indus-Yarlung Zangbo Suture Zone (IYSZ) along the Karakorum fault system (KFS), with about 1000 km of the length, a regional lithologic mapping is made using the lithologic mapping system, and the map is interpreted. The result agrees well with the known geological information and our field investigation result, although they are only available at very limited areas with relatively easy accessibility in such a hostile region of Tibet. The potential of this kind of regional scale lithologic mapping covering vast western China and surrounding region widely including Tibet, or other regions of the earth, is suggested in helping us a better recognition of the spatial distribution of typical rock types, especially ultramafic ophiolite rocks, and supplying a basic data for better understanding of the regional tectonic evolution history and the other geological topics.

ACKNOWLEDGEMENTS

This research is partially supported by METI. The ASTER data used here is supplied by ERSDAC. We are grateful to Mr. Pulong Shi and Mr. Shunhu Yang, graduate students of IGG/CAS, for their helpful support during the field investigation, and Driver Jianping Cao, who provided helpful logistic service during the field investigation.

REFERENCES

- Burg, J. P., Leyreloup, A., Girardeau, J. and Chen, G. M., 1987. Structure and metamorphism of a tectonically thickened continental crust; the Yalu Tsangpo suture zone (Tibet). *Philosophical Transactions of the Royal Society of London, Series A*, 321, 67–86.
- Corrie, R. K., Ninomiya Y., and Aitchison, J. C., 2010. Applying Advanced Spaceborne Thermal Emission and Reflection Radiometer (ASTER) spectral indices for geological mapping and mineral identification on the Tibetan plateau. *In this proceedings volume*.
- Fujisada, H., 1995. Design and performance of ASTER instrument. *P SPIE*, 2583, pp. 16-25.
- Gansser, A., 1981. The geodynamic history of the Himalaya. In: Gupta, H.K., Delany, F.M., (Eds.), *Zagros, Hindu Kush, Himalaya, Geodynamic Evolution*. American Geophysical Union Geodynamic Series 3, pp. 111–121.
- Hodges, K. V., 2000. Tectonics of the Himalaya and southern Tibet from two perspectives. *Geological Society of America Bulletin*, 112, pp. 324-350.

Molnar, P., and Tapponnier, P., 1975. Cenozoic tectonics of Asia: effects of a continental collision. *Science*, 183, pp. 419-426.

Ninomiya, Y., 2002. Mapping quartz, carbonate minerals and mafic-ultramafic rocks using remotely sensed multispectral thermal infrared ASTER data. *P SPIE*, 4710, pp. 191-202.

Ninomiya, Y., 2003. Rock type mapping with indices defined for multispectral thermal infrared ASTER data: case studies. *P SPIE*, 4886, pp. 123-132.

Ninomiya, Y., 2004. Lithologic mapping with multispectral ASTER TIR and SWIR data. *P SPIE*, 5234, pp. 180-190.

Ninomiya, Y., Fu, B., and Cudahy, T. J., 2005. Detecting lithology with Advanced Spaceborne Thermal Emission and Reflection Radiometer (ASTER) multispectral thermal infrared "radiance-at-sensor" data. *Remote Sens Environ*, 99, pp. 127-139. Corrigendum: *Remote Sens Environ*, 101, p. 567.

Tapponnier, P., Mercier, J. L., Armijo, R., Han T. and Zhou J., 1981. The Tibetan side of the India-Eurasia collision. *Nature* 294(5840), pp. 405-410

Windley, B.F., 1983. Metamorphism and tectonics of the Himalaya. *Journal of Geological Society London*, 140, pp. 849-865.

Yamaguchi, Y., Kahle, A. B., Tsu, H., Kawakami, T., and Pniel, M., 1998. Overview of Advanced Spaceborne Thermal Emission and Reflection Radiometer (ASTER). *IEEE T Geosci Remote*, 36, pp. 1062-1071.

Yin, A., Harrison, M. T., Murphy, M. A., Grove, M., Nie, S., Ryerson, F. J., Wang, X. F., Chen, Z. L., 1999. Tertiary deformation history of southeastern and southwestern Tibet during the Indo-Asian collision. *Geological Society of America Bulletin*, 111 (11), pp. 1644-1664